

# Rare $\tau$ decays

Stefano Passaggio  
 INFN, Sezione di Genova, via Dodecaneso 33, 16146 Genova, Italy

A review is presented of the current status of experimental searches for physics beyond the standard model in rare  $\tau$  decays.

## 1. Introduction

The availability of large samples of  $\tau$  leptons allows for searches of very rare (Standard Model forbidden)  $\tau$  decay modes, which provide a sensitive probe for physics beyond the Standard Model (BSM). In recent years, very large samples of  $\tau$  leptons have been made available by the high luminosity running of the two asymmetric  $B$ -factories  $PEP-II$  and KEK  $B$ , which, in light of the comparable size of the  $e^+e^- \rightarrow b\bar{b}$  and  $e^+e^- \rightarrow \tau^+\tau^-$  cross sections ( $\sigma_{\tau^+\tau^-} \sim 0.9$  nb, at  $\sqrt{s} \sim M_{\Upsilon(4S)}$ ), can rightfully be regarded as  $\tau$  factories as well. In fact, the luminosity so far recorded by the experiments  $BABAR$  and Belle running respectively at  $PEP-II$  and KEK  $B$  ( $\mathcal{L}_{BABAR} \sim 470 \text{ fb}^{-1}$ , and  $\mathcal{L}_{Belle} \sim 710 \text{ fb}^{-1}$ ) entails that the total sample of  $\tau$  pairs produced in the two experiments is already currently in excess of  $10^9$ .

Differently from the quark sector, the lepton world is well known to be characterized by an apparent remarkable conservation of flavor. An exact conservation of Lepton Flavor (LF) is naturally implemented in the Standard Model through the assumption that neutrinos are mass degenerate (actually: massless) fermions. Since the observation of neutrino oscillations, we know that the latter assumption is actually wrong, and that, with it, we also have to give up with the strict conservation of LF. However, the minimal extension of the SM that amounts to simply allowing for massive and nondegenerate neutrinos<sup>1</sup>,

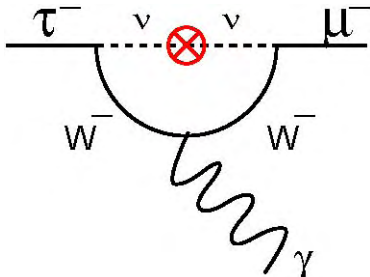


Figure 1: Dominant SM diagram contributing to the radiative LFV decay  $\tau \rightarrow \mu\gamma$ .

<sup>1</sup>I will henceforth refer to such “naïve” minimal extension of

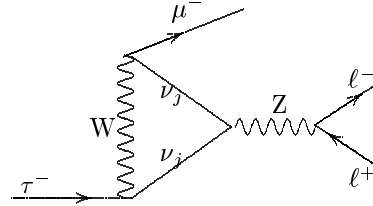


Figure 2: One loop SM diagram contributing to the non-radiative LFV decay  $\tau^- \rightarrow \mu^- l^+ l^-$  (from [4]).

due to the remarkable effectiveness of the ensuing leptonic GIM mechanism which in turn stems from the smallness of the neutrino masses, predicts extremely low rates for all LF violating (LFV) phenomena in the charged lepton sector, notwithstanding the current evidence in favor of large leptonic mixing. Using the largest value in the currently favored experimental range [1] for  $\Delta m_{32}^2 \equiv |m_3^2 - m_2^2| \sim 3 \cdot 10^{-3} \text{ eV}^2$ , where  $m_i$ ,  $i = 1, 2, 3$  are the three neutrino mass eigenvalues, and allowing for maximal mixing, the SM expected rate [2, 3] for the radiative LFV decay  $\tau \rightarrow \mu\gamma$  (see Fig. 1 for the dominant SM diagram) amounts to a surely unobservable  $\mathcal{B}(\tau^- \rightarrow \mu^- \gamma) = \frac{3\alpha}{128\pi} \left( \frac{\Delta m_{32}^2}{M_W^2} \right)^2 \sin^2 2\theta_{23} \mathcal{B}(\tau^- \rightarrow \mu^- \bar{\nu}_\mu \nu_\tau) \sim 10^{-54}$ .

It is worthwhile to remark that the SM suppression of LFV processes in the charged sector, though a general feature of the model, doesn’t achieve to the same degree, and in particular to the extreme one mentioned above, for all processes. As noted by Pham [4], LFV  $\tau$  decays of the kind of  $\tau^- \rightarrow \mu^- l^+ l^-$  or  $\tau^- \rightarrow \mu^- \rho^0$  ( $l = e, \mu$ ), due to the presence of infrared divergences in the contributing diagram shown in Fig. 2, get in fact a milder, logarithmic, suppression factor in place of the striking factor  $(\Delta m_{ij}^2/M_W^2)^2$  suppressing the class of radiative LFV processes  $\tau \rightarrow l\gamma$ . The SM prediction for the rate of such nonradiative LFV processes turns in fact to be proportional

the Standard Model as “SM”, without further comments upon it actually being an extension of the Standard Model proper. It amounts to simply extending the Standard Model by the addition of an appropriate neutrino mass matrix in a gauge invariant manner, while keeping the minimal Higgs scheme, with only one Higgs doublet.

to  $\sum_{k=2}^3 U_{\tau k} U_{\mu k}^* \ln \frac{m_k^2}{m_1^2}$ . Taking into account the current experimental knowledge on neutrino mixing, this translates to expected branching ratios many orders of magnitude larger than those expected for  $\tau \rightarrow l\gamma$  (Pham [4] estimates  $\mathcal{B} \gtrsim 10^{-14}$ ), but in any case far below the current experimental reach.

The above considerations allow us to draw two important conclusions. The first one is that, although the discovery that neutrinos are massive entails that LF numbers are no longer conserved in the SM, we can safely state that, as long as the SM represents the correct physical description, no LFV process in the charged sector (CLFV) should ever be observed. This means that observation of CLFV would undoubtedly be a signature of BSM physics. The second conclusion is that it is worthwhile and important to search for CLFV in all possible experimentally searchable processes (e.g. radiative and nonradiative ones), since: (a) as shown to be the case in the SM, also in most BSM physics scenarios different CLFV processes could be characterized by widely different rates, and (b) the eventual observation and measurement of LFV in different processes can be generally expected to be sensitive to different sectors of the new physics parameter space and better constraining the choice of a new scenario.

In fact, many scenarios of BSM physics predict rates for LFV  $\tau$  decays that are not too far, or even within, the current experimental reach. Without pretending to be exhaustive, table I shows some examples of scenarios that have been theoretically investigated, with the corresponding order of magnitude expectations for the branching ratio of radiative and nonradiative LFV  $\tau$  decays.

Table I Examples of BSM scenarios predicting rates of LFV  $\tau$  decays not too far, or even within, the current experimental reach. Order of magnitude expectations for the two broad classes of radiative (e.g.  $\tau \rightarrow l\gamma$ ) and nonradiative (e.g.  $\tau \rightarrow 3l$ ) LFV  $\tau$  decays are displayed in the last two columns.

	$\mathcal{B}(\tau \rightarrow l\gamma)$	$\mathcal{B}(\tau \rightarrow 3l)$
SUSY Higgs [5, 6]	$10^{-10}$	$10^{-7}$
SM + Heavy Majorana $\nu_R$ [7]	$10^{-9}$	$10^{-10}$
Non-universal $Z'$ [8]	$10^{-9}$	$10^{-8}$
SUSY $SO(10)$ [9, 10]	$10^{-8}$	$10^{-10}$
mSUGRA + Seesaw [11, 12]	$10^{-7}$	$10^{-9}$

## 2. Searching for LFV $\tau$ decays at $e^+e^-$ colliders

The *BABAR* [13] and Belle [14] detectors are remarkably similar, with the major difference being

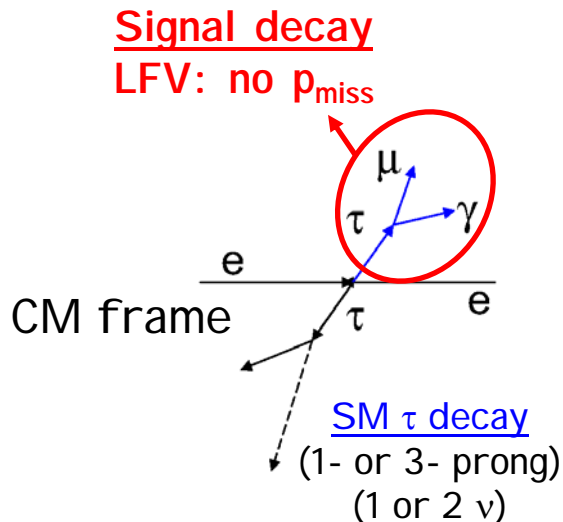


Figure 3: Schematic drawing of the production of  $\tau$  pairs in  $e^+e^-$  collisions, displayed in the CM frame. The figure also illustrates the general strategy employed in searches for LFV  $\tau$  decays at  $e^+e^-$  colliders: one  $\tau$  is reconstructed in a SM allowed (“Tag”) decay, characterized by a 1- or 3-prong + 1 or 2  $\nu$  final state, while the search for a possible LFV (neutrinoless!) decay is performed on the recoiling (“Signal”)  $\tau$ .

in the technology used to identify charged particles: Belle uses a threshold Čerenkov detector together with time-of-flight and tracker  $dE/dx$ , whereas *BABAR* mainly relies on a ring-imaging Čerenkov detector augmented by  $dE/dx$  in the trackers.

In addition to the statistics issue already discussed in the introduction,  $e^+e^-$  colliders running at, or nearby, the  $\Upsilon(4S)$  resonance provide a very clean environment for the search of rare (and, in particular, LFV)  $\tau$  decays.  $\tau$  leptons are exclusively<sup>2</sup> produced in pairs through the QED process  $e^+e^- \rightarrow \tau^+\tau^-$ , and thereby fly back-to-back in the  $e^+e^-$  Center of Mass (CM) frame (Fig. 3). At the asymmetric *B*-factories *PEP-II* and *KEK B* the events are boosted in the laboratory (Lab) frame with a  $\beta\gamma \simeq 0.56$  for the *BABAR* experiment and  $\simeq 0.43$  for Belle. The boost of each of the two  $\tau$ 's in the CM frame, combined with such a CM-to-Lab boost, confer to the final state of each  $\tau$  decay a “jet-like” shape which allows not only to powerfully reject the  $B\bar{B}$  background, but also to easily separate the final state products of one  $\tau$  from those of the other.

The general strategy employed in searches for LFV  $\tau$  decays at  $e^+e^-$  colliders consists in searching for  $e^+e^- \rightarrow \tau^+\tau^-$  events where one  $\tau$  is reconstructed in a SM allowed decay (henceforth referred to as “Tag”

<sup>2</sup>Apart from possible initial or final state radiation  $\gamma$ '(s).

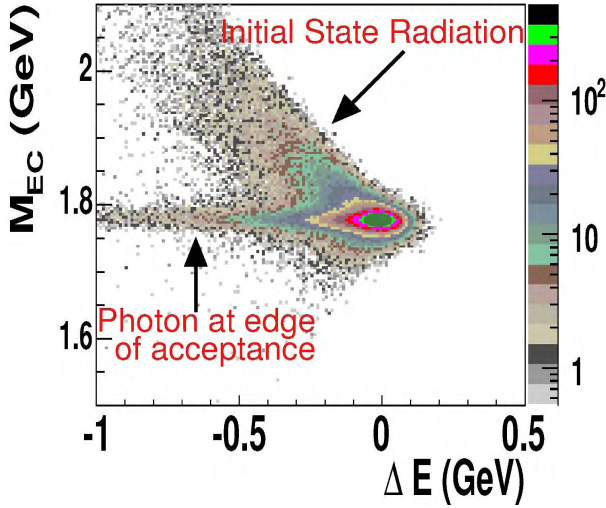


Figure 4: Scatter plot of the reconstructed variables  $M_{\text{LFVD}}$  and  $\Delta E$  for MC simulated  $e^+e^- \rightarrow \tau^+\tau^-$  events where one of the  $\tau$  leptons decays to the LFV final state  $\mu\gamma$  (from the *BABAR* experiment). For the exact meaning of the variable plotted along the vertical axis ( $M_{\text{EC}}$ ), see the text and footnote 3. The dark green ellipse drawn on top of the distribution in correspondence of the constraints expressed by Eqs. 1 and 2 illustrates in a qualitative fashion the relative size of a typical 2 – 3 standard deviations wide signal box employed in the final event selection.

decay), characterized by a 1- or 3-prong + 1 or 2  $\nu$  final state, while the search for a possible LFV decay (LFVD) is performed on the recoiling (“Signal”)  $\tau$ . A noteworthy feature of all LFV  $\tau$  decays searched for by *BABAR* and Belle is that such decays do not bear any undetectable particle (specifically: any neutrino) in their final state, and can therefore be completely reconstructed. In other words, the observed missing momentum of the reconstructed complete event is wholly attributable to the “Tag” decay. This circumstance provides very powerful tools for background rejection, which amount to requesting that the reconstructed invariant mass and CM energy for the candidate LFVD (“Signal”) side of the event coincide with the nominal mass of the  $\tau$  lepton and with half the CM energy of the  $e^+e^-$  collision, respectively:

$$M_{\text{LFVD}} = m_\tau \quad (1)$$

$$\Delta E \equiv E_{\text{LFVD}}^{\text{CM}} - \frac{\sqrt{s}}{2} = 0 \quad (2)$$

An example of the distribution of simulated signal ( $\tau \rightarrow \mu\gamma$ ) MC events in a scatter plot of these two kinematical variables is shown in Fig. 4, which displays the accumulation of signal events in correspondence of the two constraints given by Eqs. 1 and 2, as well as the smearing brought about by resolution and radiative effects, respectively. The same figure displays also in a qualitative fashion a two dimensional

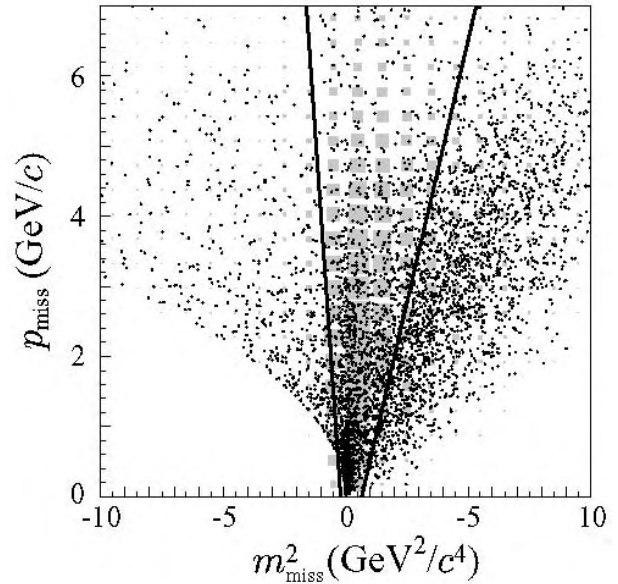


Figure 5: Scatter plot of the reconstructed variables  $p_{\text{miss}}$  and  $m_{\text{miss}}^2$  for data (dots) and signal MC (shaded boxes) events in a search for the LFV decay  $\tau \rightarrow \mu\gamma$  by the Belle collaboration [18]. The selection criterion employed consists in requiring that the event lies between the two lines in the figure.

signal box which is used to separate the signal from the SM backgrounds.

Exploiting at best the available constraints can significantly boost the sensitivity of the search. An example of this important remark is offered by the strategy employed by the *BABAR* experiment since the publication of their search for  $\tau \rightarrow \mu\gamma$  decays [15]. The choice of evaluating  $M_{\text{LFVD}}$  by imposing a beam energy constraint<sup>3</sup>, obtained by fixing the “Signal”  $\tau$  decay vertex – or equivalently the emission point of the photon in the final state – in correspondence of the point of closest approach of the signal  $\mu$  trajectory to the beam axis, brought a dramatical improvement in terms of resolution on such a kinematical variable<sup>4</sup> with respect to a more straightforward reconstruction of the same quantity as an unconstrained invariant mass of the LFVD decay products. Typical values for the resolution on the other kinematical quantity  $\Delta E$  range around  $\sim 50$  MeV.

Other ingredients crucial to an effective reduction of backgrounds consist in a clever use of the powerful

<sup>3</sup>Whence the use of the symbol  $M_{\text{EC}}$  in the scatter plot of Fig. 4.

<sup>4</sup>The resolution improvement on  $M_{\text{LFVD}}$  due to the beam energy constraint technique ( $M_{\text{EC}}$ ) is greater of a factor two:  $\sigma(M_{\text{EC}}) \sim 9$  MeV, while  $\sigma(M_{\text{inv}}) \sim 20$  MeV, where  $M_{\text{inv}}$  denotes the straightforward evaluation of the kinematical quantity  $M_{\text{LFVD}}$  as an unconstrained invariant mass of the LFVD decay products.

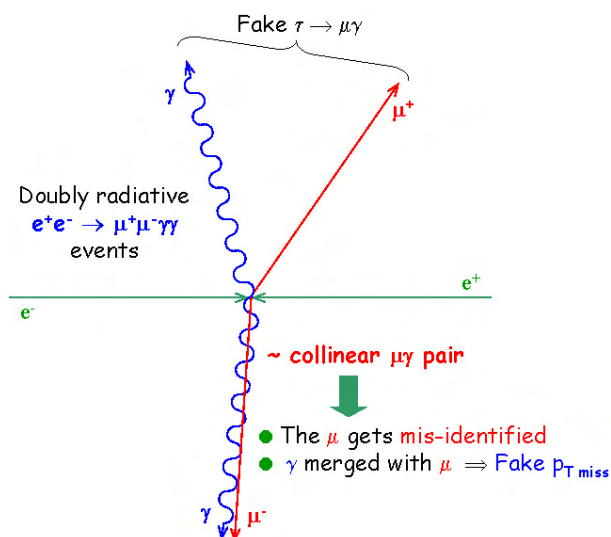


Figure 6: Schematic representation of a doubly radiative,  $e^+e^- \rightarrow \mu^+\mu^-\gamma\gamma$ , fake missing momentum event.

particle identification capabilities of the two experiments and, whether possible, in the exploitation of additional constraints on the event. An example of the latter strategy is represented by the requirement that the reconstructed event missing mass ( $m_{\text{miss}}$ ), when the “Tag” decay is chosen so as to have a single neutrino in the final state, be compatible with zero. Such a constraint proved to be very effective in Belle’s searches for the LFV decay  $\tau \rightarrow \mu\gamma$  [18], as illustrated in Fig. 5, where the selection criterion on  $m_{\text{miss}}^2$  employed by the Belle collaboration is seen to be implemented in a  $p_{\text{miss}}$ -dependent fashion.

In addition, a rewarding strategy has in some cases turned out to consist in trying to identify, and then cleverly fight, specific, particularly nasty, backgrounds which could otherwise survive all other selection criteria. An example of this situation is represented by a fraction of the residual  $\mu\mu\gamma(s)$  background in searches for the  $\tau \rightarrow \mu\gamma$  decay, namely that consisting of doubly (or more) radiative events where the flight path of one of the photons lies sufficiently close to the trajectory of the charged track in the “Tag” side of the event. In these occurrences, schematically illustrated in Fig. 6, such a photon may fail to be reconstructed as a neutral cluster in the electromagnetic calorimeter and its energy deposit in the calorimeter could eventually get associated to the nearby charged track. When the photon is sufficiently energetic, such occurrences would mimic a substantial missing momentum. Concurrently, the “Tag” side charged track would erroneously fail to be identified as a muon according to basically any of the standard  $\mu$  identification criteria because of the large energy deposit in the calorimeter erroneously associated to it.

As a general rule, both *BABAR* and Belle optimize<sup>5</sup> their selection strategy, and the particular values of the associated cuts, by using samples of fully simulated and reconstructed signal and background MC events. MC samples, possibly checked with control samples or with data events sufficiently far from the signal region (sidebands), are also used to model the background shapes of relevant kinematical variables for the purpose of estimating and subtracting the final background contribution, whose normalization is obtained from sidebands data. The MC simulation of the signal is also used to determine the signal efficiency ( $\epsilon$ ), which typically lies between 2% and 10%, depending on the channel under study. To minimize possible biases, both experiments adopt a blind analysis approach, which consists in excluding from consideration, up to the moment when the full selection and all systematic studies are completely finalized, all events in the data within a suitably shaped and sized region in the  $M_{\text{LFVD}}$  and  $\Delta E$  plane around the signal signature values given by Eqs. 1 and 2.

In order to possibly boost the sensitivity of the search, the two experiments have adopted a spectrum of different approaches to finally discriminate a possible signal from the residual background and obtain an estimate of the former’s size: these range from simple cut-and-count to likelihood techniques, and in one case a Neural-Network selection has been adopted. If the estimated background ( $N_{\text{bkd}}$ ) is compatible with the observed number of events, a 90% confidence level (CL) upper limit on the number of signal events is estimated<sup>6</sup> ( $N_{90}^{\text{UL}}$ ). Based on this quantity and on the estimate of the signal efficiency  $\epsilon$ , a 90% CL upper limit on the branching ratio is obtained as:

$$\mathcal{B}_{90}^{\text{UL}} = \frac{N_{90}^{\text{UL}}}{2\mathcal{L}\sigma_{\tau+\tau}-\epsilon}. \quad (3)$$

### 3. Experimental results

Both *BABAR* and Belle have searched for LFV in many different classes of  $\tau$  decays. In the following I’ll summarize the results obtained by the two experiments, grouping them according to the decay final state searched for and giving particular emphasis only to the most recent ones.

<sup>5</sup>The analyses are optimized to give the best “expected upper limit”.

<sup>6</sup>Also in this respect, the two experiments have resorted to a number of different techniques [16, 17]. It should be noted that the experimental upper limits quoted by both the experiments are in any case of a frequentistic nature. Negative fluctuations are generally admitted (and occur!) and give rise to “measured” upper limits that can be substantially lower than the “sensitivity” or “expected upper limit” of the corresponding search.

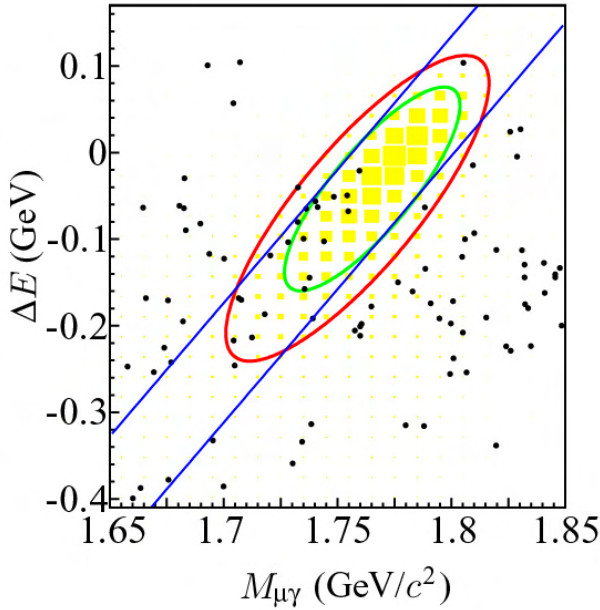


Figure 7: Scatter plot of the reconstructed variables  $\Delta E$  and  $M_{LFVD}$  for the final event selection obtained in the most recent Belle search for  $\tau \rightarrow \mu\gamma$ . Dots are data events and yellow squares represent MC signal events. The inner green ellipse is the  $2\sigma$  signal region (where a total of 10 data events are observed, with an estimated efficiency  $\epsilon = 5.1\%$ ), while the outer red ellipse is the  $3\sigma$  blinded region.

### 3.1. Search for $\tau \rightarrow l\gamma$ ( $l = e, \mu$ )

The most recent  $\tau \rightarrow \mu\gamma$  and  $\tau \rightarrow e\gamma$  results were submitted for publication by Belle [18] using a data sample corresponding to a luminosity  $\mathcal{L} = 535 \text{ fb}^{-1}$ . The  $\tau \rightarrow \mu\gamma$  ( $\tau \rightarrow e\gamma$ ) analyses have a 5.1% (3.0%) signal efficiency within a 2D elliptical signal region in the  $M_{LFVD}$  and  $\Delta E$  plane (see Fig. 7 and Fig. 8).

After performing a 2D unbinned extended maximum likelihood fit for the number of signal ( $s$ ) and background ( $b$ ) events, Belle finds  $s = -3.9_{-3.2}^{+3.6}$  ( $-0.14_{-2.45}^{+2.18}$ ) and  $b = 13.9_{-4.8}^{+6.0}$  ( $5.14_{-2.81}^{+3.86}$ ) in the  $\tau \rightarrow \mu\gamma$  ( $\tau \rightarrow e\gamma$ ) search. Toy MC simulations are then used to evaluate the probability of obtaining such results<sup>7</sup> and to estimate the 90% CL upper limits on the number of signal events:  $N_{90}^{UL}(\tau \rightarrow \mu\gamma) = 2.0$  and  $N_{90}^{UL}(\tau \rightarrow e\gamma) = 3.3$ . The branching ratio upper limits following from these results amount respectively to  $\mathcal{B}(\tau \rightarrow \mu\gamma) < 4.5 \cdot 10^{-8}$  and  $\mathcal{B}(\tau \rightarrow e\gamma) < 1.2 \cdot 10^{-7}$  at 90% CL.

The corresponding limits previously obtained by BABAR on  $\mathcal{L} = 211 \text{ fb}^{-1}$  amount to  $\mathcal{B}(\tau \rightarrow \mu\gamma) < 6.8 \cdot 10^{-8}$  [15] and  $\mathcal{B}(\tau \rightarrow e\gamma) < 1.1 \cdot 10^{-7}$  [19] at 90%

<sup>7</sup>Belle evaluates that  $P(s \leq -3.9) = 25\%$  ( $P(s \leq -0.14) = 48\%$ ) for null true signal in the  $\tau \rightarrow \mu\gamma$  ( $\tau \rightarrow e\gamma$ ) search.

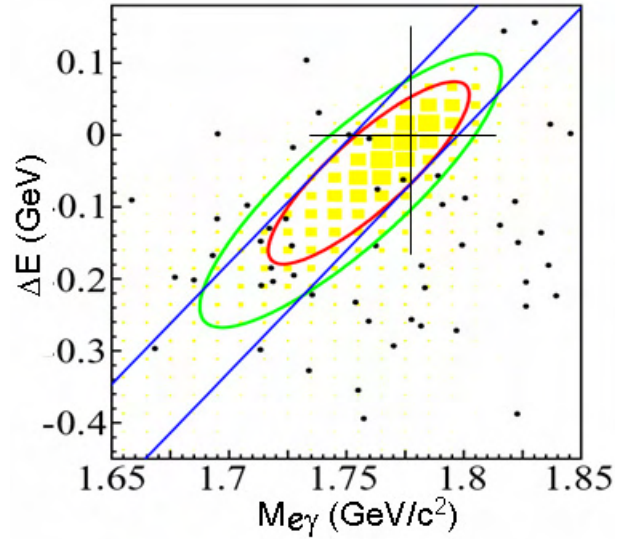


Figure 8: Scatter plot of the reconstructed variables  $\Delta E$  and  $M_{LFVD}$  for the final event selection obtained in the most recent Belle search for  $\tau \rightarrow e\gamma$ . Dots are data events and yellow squares represent MC signal events. The inner red ellipse is the  $2\sigma$  signal region (where a total of 5 data events are observed, with an estimated efficiency  $\epsilon = 3.0\%$ ), while the outer green ellipse is the  $3\sigma$  blinded region.

CL.

Fig. 9 summarizes and compares the BABAR and Belle results discussed above, and the corresponding analyzed luminosities.

### 3.2. Search for $\tau \rightarrow l\pi^0, l\eta, l\eta', lK_S^0$

Both BABAR [20] and Belle [21] have recently published new results on LFV  $\tau$  decays involving the  $\pi^0$ ,  $\eta$  and  $\eta'$  pseudoscalars:  $\tau \rightarrow l\pi^0, l\eta, l\eta'$ , where  $l$  is separately identified as either an electron or a muon. The luminosity analyzed by BABAR is  $\mathcal{L} = 339 \text{ fb}^{-1}$ , while Belle used  $\mathcal{L} = 401 \text{ fb}^{-1}$ . In the modes with an  $\eta$  meson in the final state both the  $\eta \rightarrow \gamma\gamma$  and the  $\eta \rightarrow \pi^+\pi^-\pi^0$  decays are used. In the  $\tau \rightarrow l\eta'$  analyses the  $\eta' \rightarrow \pi^+\pi^-\eta$  ( $\eta \rightarrow \gamma\gamma$ ) and  $\eta' \rightarrow \rho^0\gamma$  decay modes were included. Fig. 10 shows the distribution of the finally selected data events in the  $M_{LFVD}$  and  $\Delta E$  plane for each of these channels, together with the  $2\sigma$  signal box used in the BABAR search.

The BABAR expected background per channel is between 0.1 and 0.3 events. Summing over all ten modes, the total expected background within the signal regions amounts to 3.1 events, whereas 2 events in total were observed.

Belle had previously published a search for an additional mode with a neutral pseudoscalar meson in the final state ( $\tau \rightarrow lK_S^0$  [22],  $\mathcal{L} = 281 \text{ fb}^{-1}$ ).

Fig. 11 summarizes and compares the BABAR and Belle results on all searches for  $\tau$  LFV decays to a

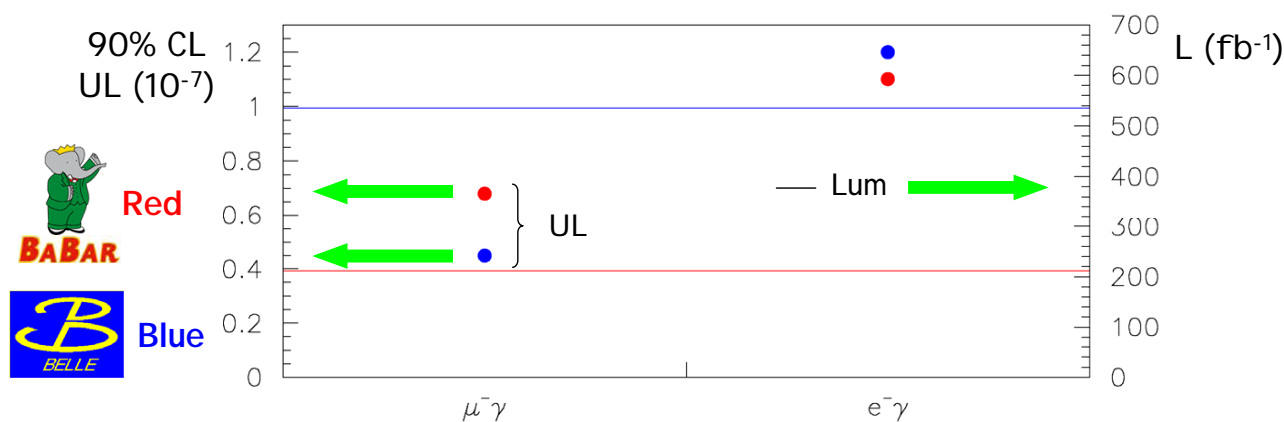


Figure 9: Summary and comparison of the current upper limits (dots: left vertical axis) set by *BABAR* (red) and Belle (blue) on  $\mathcal{B}(\tau \rightarrow \mu\gamma)$  and  $\mathcal{B}(\tau \rightarrow e\gamma)$ . The corresponding analyzed luminosities are shown as horizontal lines on a scale displayed on the right vertical axis.

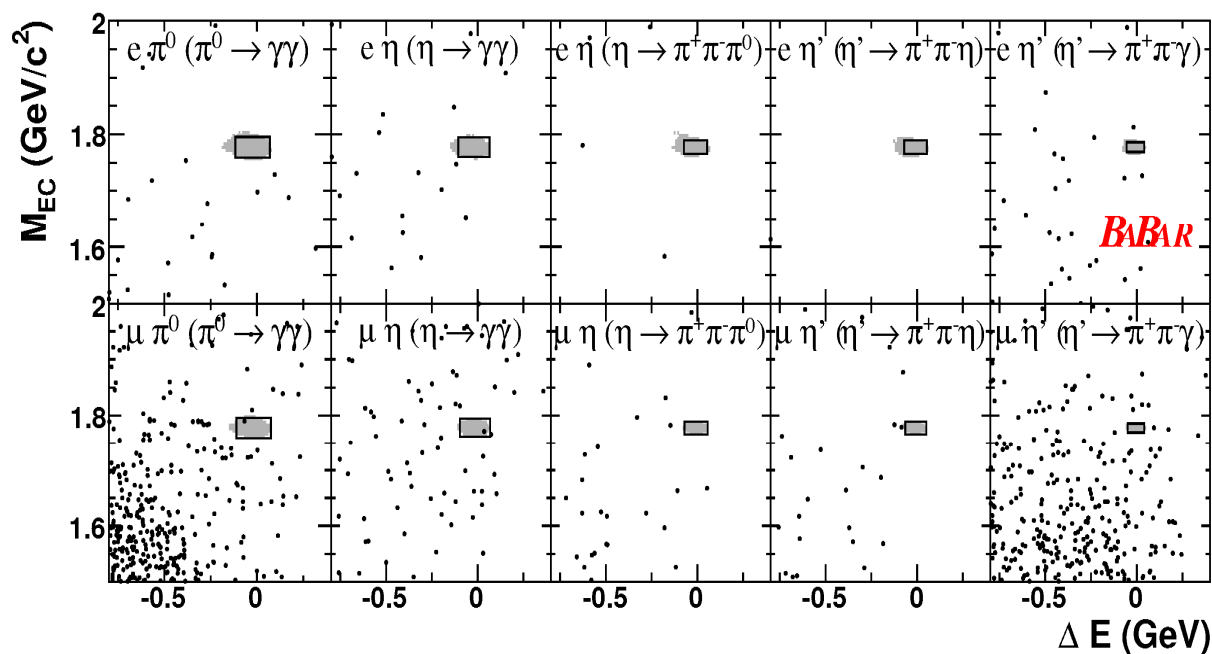


Figure 10: Selected data (dots) and 68% of signal MC events (shaded region) in the  $M_{\text{LFVD}}$  and  $\Delta E$  plane for the 10 LFV decay channels  $\tau \rightarrow l\pi^0, l\eta, l\eta'$  searched for by *BABAR*; for each channel, the corresponding  $2\sigma$  signal box is displayed.

lepton and a neutral pseudoscalar meson.

of decays  $\tau \rightarrow 3l$  [25, 26]<sup>8</sup>, while Fig. 14 shows the results published by Belle on several  $\tau$  decays to a lepton and a neutral vector meson [24].

### 3.3. Other searches for $\tau$ LFV decays

Both *BABAR* and Belle have searched for other  $\tau$  LFV decays. The corresponding results are compared in Fig. 12 for the class of decays  $\tau \rightarrow lh h'$  (where  $h$  and  $h' = \pi^\pm$  or  $K^\pm$ ) [23, 24]. Fig. 13 compares the results obtained by the two experiments for the class

<sup>8</sup>*BABAR* has very recently submitted for publication [27] an updated search for  $\tau \rightarrow 3l$ , using a much larger luminosity ( $\mathcal{L} = 376 \text{ fb}^{-1}$ ) than previously published by each of the two experiments (see Fig. 13). Upper limits on the branching fractions are set in the range  $(4-8) \cdot 10^{-8}$  at 90% CL. These results were not public when FPCP2007 took place, and were not presented at the Conference.

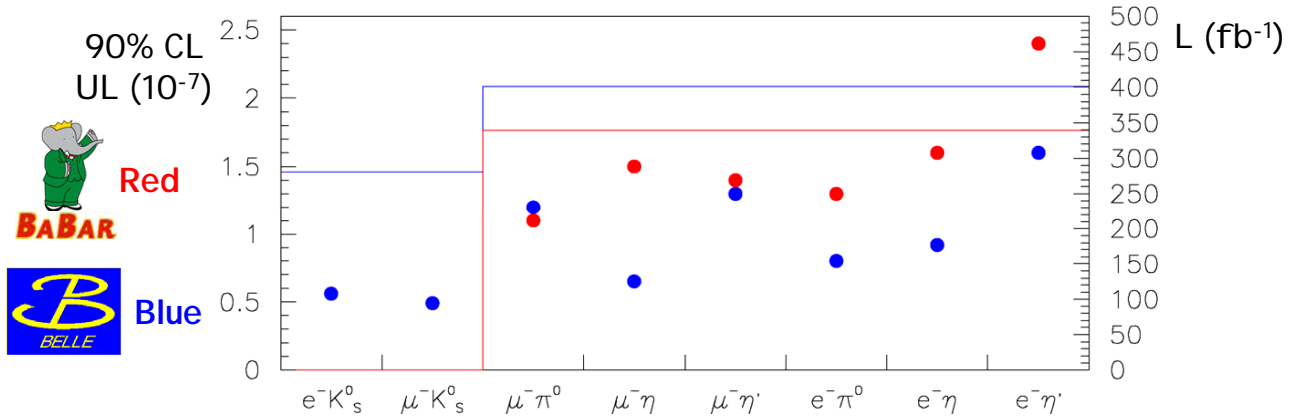


Figure 11: Summary and comparison of the current upper limits (dots: left vertical axis) set by *BABAR* (red) and Belle (blue) on the branching ratios for  $\tau$  decays to a lepton and a neutral pseudoscalar meson. The corresponding analyzed luminosities are shown as horizontal lines on a scale displayed on the right vertical axis.

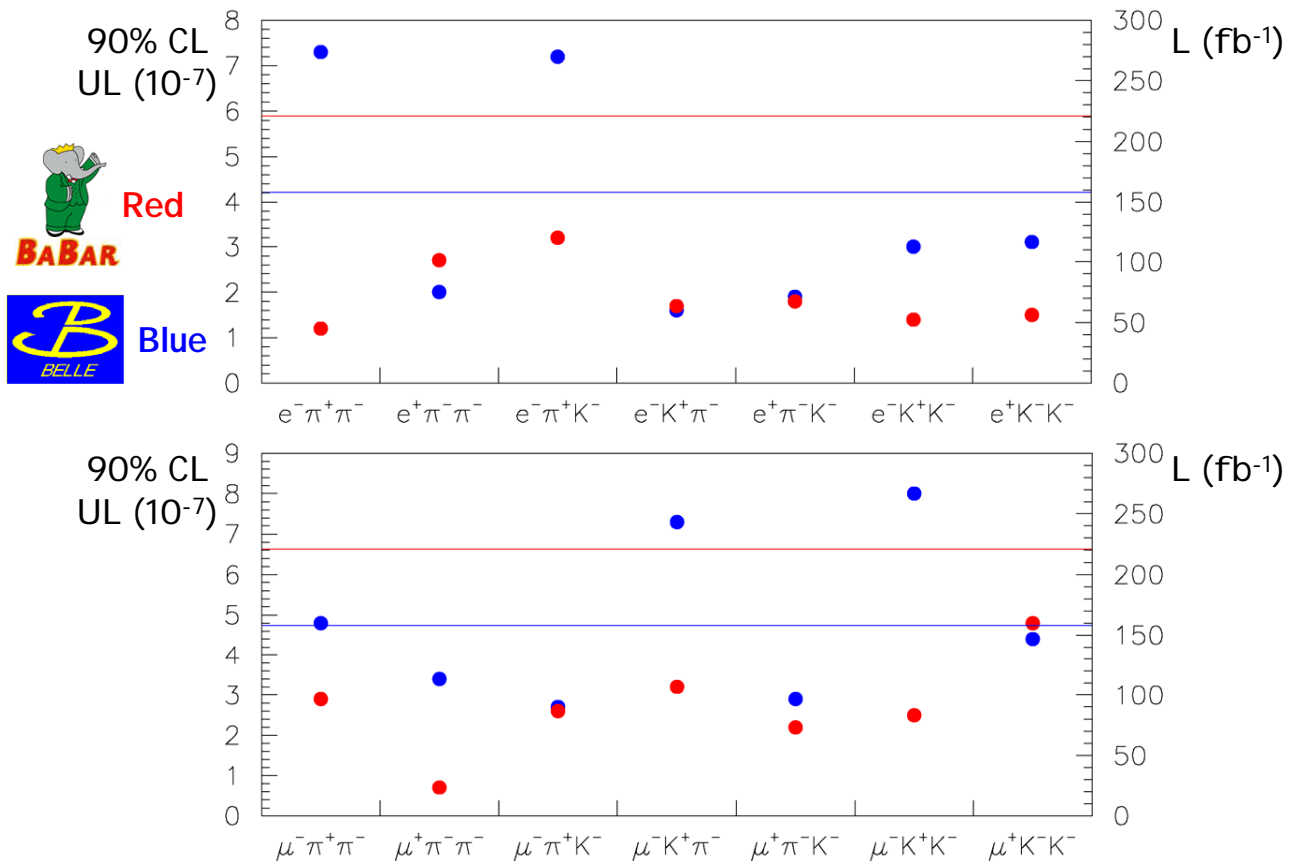


Figure 12: Summary and comparison of the current upper limits (dots: left vertical axis) set by *BABAR* [23] (red) and Belle [24] (blue) on the branching ratios for  $\tau$  decays to a lepton and a pair of charged pseudoscalar mesons. The corresponding analyzed luminosities are shown as horizontal lines on a scale displayed on the right vertical axis.

#### 4. Future Prospects for LFV searches in $\tau$ decays

The estimated physics reach of the full data sample that will be collected by *BABAR* and Belle till the

end of their foreseen running, based on projections from existing analyses, depends on the residual background level. We express the experimental reach in terms of the “expected 90% CL upper limit” and, for brevity’s sake, refer to this as the “sensitivity”. In the absence of signal, for large  $N_{\text{bkd}}$ ,  $N_{90}^{UL} \sim 1.64N_{\text{bkd}}$ ,

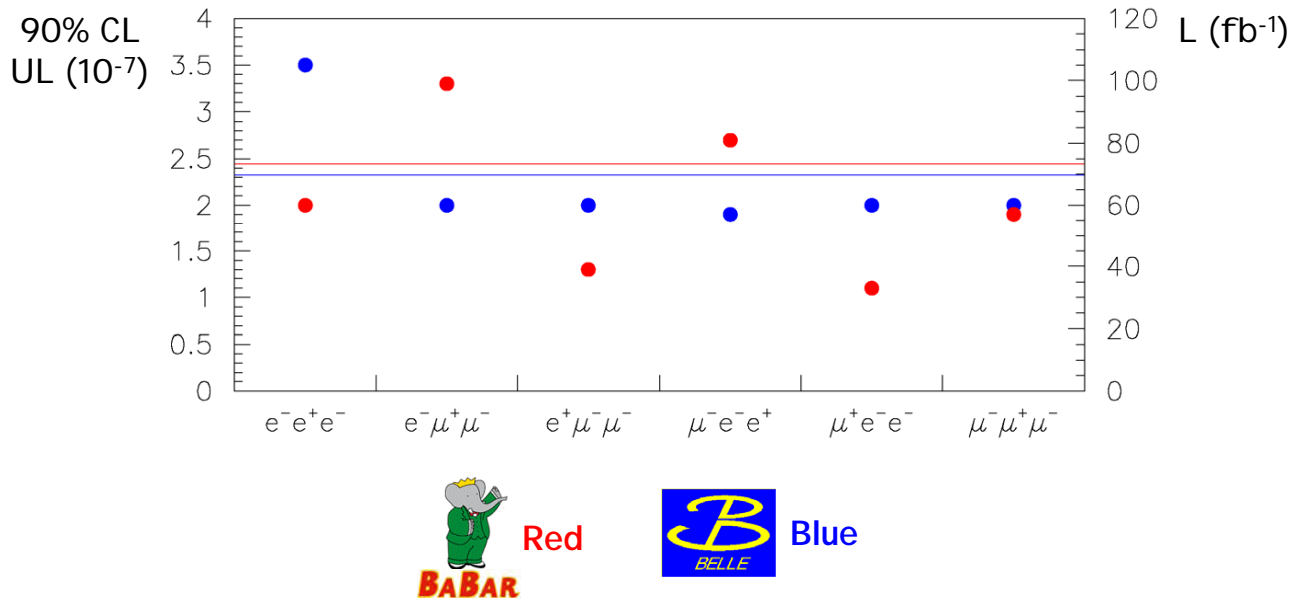


Figure 13: Summary and comparison of the current published upper limits (dots: left vertical axis) set by *BABAR* [25] (red) and Belle [26] (blue) on the branching ratios for  $\tau$  decays to three charged leptons. The corresponding analyzed luminosities are shown as horizontal lines on a scale displayed on the right vertical axis.

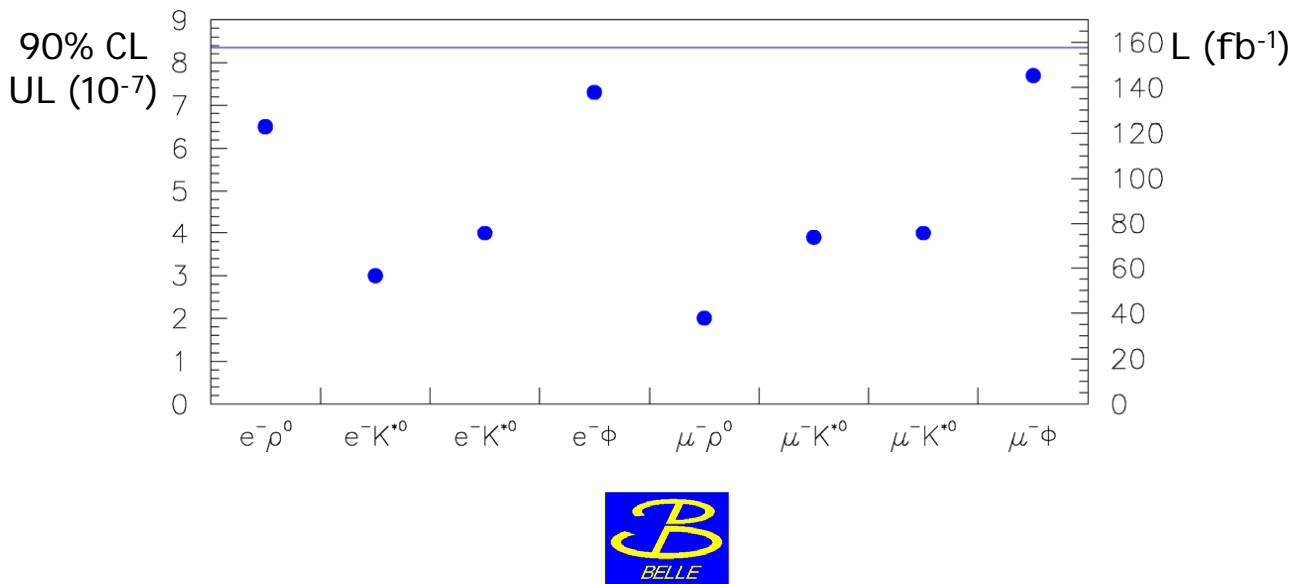


Figure 14: Summary of the current upper limits (dots: left vertical axis) set by Belle [24] on the branching ratios for  $\tau$  decays to a lepton and a neutral vector meson. The corresponding analyzed luminosity is shown as a horizontal line on the scale displayed on the right vertical axis.

whereas for small  $N_{\text{bkd}}$  a value for  $N_{90}^{UL}$  is obtained using the method described in [28]. So, for  $N_{\text{bkd}} \sim 0$ ,  $N_{90}^{UL} \sim 2.4$ . Reducing the background below a handful of events doesn't greatly improve the expected limit if significant efficiency is lost in the process, which is why it is common to see experiments reporting the expected backgrounds to be small (i.e. a few events), but rarely below 0.1 of an event.

A worst-case scenario is obtained if identical analyses to those already published by *BABAR* and Belle are repeated, as is, on the increased data sample: in that case the expectations then simply scale as  $\sqrt{N_{\text{bkd}}}/\mathcal{L}$ , which, for large  $N_{\text{bkd}}$ , scales as  $1/\sqrt{\mathcal{L}}$ . A best case scenario would take the current expected limit and scale it linearly with the luminosity. This is equivalent to a statement that analyses can be developed



maintaining the same efficiency and backgrounds as the current analyses.

For  $\tau \rightarrow l\gamma$ , there is an irreducible background from  $\tau \rightarrow l\nu\nu$  for  $e^+e^- \rightarrow \tau^+\tau^-$  events accompanied by initial state radiation (ISR). The ISR photon can be combined with the lepton  $l$  to form a  $\tau \rightarrow l\gamma$  candidate that accidentally falls in the signal region in the  $M_{\text{LFVD}} - \Delta E$  plane. Such a background is irreducible in the sense that it arises from an  $e^+e^- \rightarrow \tau^+\tau^-$  process with a well measured lepton and  $\gamma$  in one of the  $\tau$  hemispheres. In the existing *BABAR* analyses, these events account for approximately one fifth of the total residual background. Scaling with this irreducible background only, one would expect an upper limit for  $\mathcal{B}(\tau \rightarrow l\gamma)$  which ranges between 1 and  $2 \cdot 10^{-8}$  from a complete combined *BABAR* and Belle data set.

The situation for the other LFV decays,  $\tau \rightarrow 3l$  and  $\tau \rightarrow lhh'$ , is even more promising, since these modes do not suffer from the aforementioned backgrounds from ISR. In this case, one can project sensitivities assuming  $N_{\text{bkd}}$  comparable to backgrounds in existing analyses for approximately the same efficiencies. These yield expected limits at the  $10^{-8}$  level with the complete *BABAR* and Belle data set.

## 5. Conclusions

Searches for LFV in  $\tau$  decays are an optimal hunting ground for BSM physics, which is complementary to possible LHC discoveries: observation or non observation of LFV processes in the charged sector can significantly constrain theory parameter space.

*BABAR* and Belle have looked for signals of LFV in many exclusive  $\tau$  decay modes and, although no evidence of LFV has yet been found, limits have pushed into the  $10^{-8}$  region where parameter space in some BSM scenarios is already being constrained. An example of the constraining power of the current experimental limits is shown in Fig. 15, where the *BABAR* and Belle limits on  $\mathcal{B}(\tau \rightarrow \mu\gamma)$  are superimposed to a scatter plot of theoretical predictions obtained in a SUSY  $SO(10)$  scenario of BSM physics [9]. Also shown for comparison is the best experimental limit available in the pre-asymmetric-*B*-factory era.

It should finally be mentioned that there exist proposals [29] for Super *B*-factories which would generate up to a 100 fold increase in the size of the  $\tau$  sample compared to those expected from the existing *B*-factories. If such a facility is built, one will be probing LFV  $\tau$  decays at the  $O(10^{-9} \rightarrow 10^{-10})$  level.

## Acknowledgments

I wish to warmly thank the organizers for the great conference and G. Ridolfi for carefully reading the manuscript.

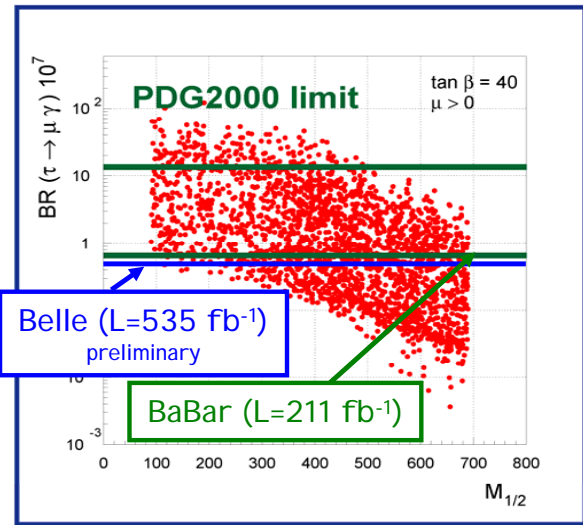


Figure 15: *BABAR* and Belle current experimental limits on  $\mathcal{B}(\tau \rightarrow \mu\gamma)$  compared to a range of theoretical predictions for this branching ratio in a SUSY  $SO(10)$  scenario of BSM physics [9]. The best experimental limit available before the two asymmetric *B*-factories started to play a role is shown by the uppermost dark green horizontal line (“PDG2000 limit”).

## References

- [1] W. M. Yao et al. (Particle Data Group), J. Phys. **G 33** (2006) 1, and 2007 partial update for edition 2008 (<http://pdg.lbl.gov/>)
- [2] B. W. Lee, R. E. Shrock, Phys. Rev. D **16** (1977) 1444
- [3] T. P. Cheng, L.-F. Li, Phys. Rev. Lett. **45** (1980) 1908
- [4] X.-Y. Pham, Eur. Phys. Jour. C **8** (1999) 513
- [5] A. Dedes, J. Ellis, M. Raidal, Phys. Lett. B **549** (2002) 159
- [6] A. Brignole, A. Rossi, Phys. Lett. B **566** (2003) 517
- [7] G. Cvetic, C. Dib, C. S. Kim, J. D. Kim, Phys. Rev. D **66** (2002) 034008
- [8] C. Yue, Y. Zhang, L. Liu, Phys. Lett. B **547** (2002) 252
- [9] A. Masiero, S. Vempati, O. Vives, Nucl. Phys. B **649** (2003) 189 and New J. of Phys. **6** (2004) 202
- [10] T. Fukuyama, T. Kikuchi, N. Okada, Phys. Rev. D **68** (2003) 033012
- [11] J. Ellis, M. E. Gómez, G.K. Leontaris, S. Lola, D. V. Nanopoulos, Eur. Phys. Jour. C **14** (2000) 319
- [12] J. Ellis, J. Hisano, M. Raidal, Y. Shimizu, Phys. Rev. D **66** (2002) 115013
- [13] B. Aubert et al. (*BABAR* collaboration), Nucl. Instr. Methods Phys. Res., Sect. A **479** (2002) 1

- [14] A. Abashian et al. (Belle collaboration), Nucl. Instr. Methods Phys. Res., Sect. A **479** (2002) 117
- [15] B. Aubert et al. (*BABAR* collaboration), Phys. Rev. Lett. **95** (2005) 041802
- [16] I. Narsky, Nucl. Instr. Methods Phys. Res., Sect. A **450** (2000) 444
- [17] T. Junk, Nucl. Instr. Methods Phys. Res., Sect. A **434** (1999) 435; A. L. Read, J. Phys. **G 28** (2002) 2693; these references are relative to the so called “modified frequentistic” (or  $CL_S$ ) method, which at least partially addresses the issue raised in footnote 6 with the goal of reducing the occurrence of wrong results due to a possible overestimation of the background; such approach has been adopted in one of the two flavors of the *BABAR* search for  $\tau \rightarrow \mu\gamma$  described in Ref. [15], albeit in a frequentistic ( $CL_{S+B}$ ) fashion, in order to harmonize with the flavor of all the other quoted experimental results.
- [18] K. Hayasaka et al. (Belle collaboration), Belle preprint 2007-6 and [arXiv:0705.0650](https://arxiv.org/abs/0705.0650) [[hep-ex](#)], submitted to Phys. Lett. B
- [19] B. Aubert et al. (*BABAR* collaboration), Phys. Rev. Lett. **96** (2006) 041801
- [20] B. Aubert et al. (*BABAR* collaboration), Phys. Rev. Lett. **98** (2007) 061803
- [21] Y. Miyazaki et al. (Belle collaboration), Phys. Lett. B **648** (2007) 341
- [22] Y. Miyazaki et al. (Belle collaboration), Phys. Lett. B **639** (2006) 159
- [23] B. Aubert et al. (*BABAR* collaboration), Phys. Rev. Lett. **95** (2005) 191801
- [24] Y. Yusa et al. (Belle collaboration), Phys. Lett. B **640** (2006) 138
- [25] B. Aubert et al. (*BABAR* collaboration), Phys. Rev. Lett. **92** (2004) 121801
- [26] Y. Yusa et al. (Belle collaboration), Phys. Lett. B **589** (2004) 103
- [27] B. Aubert et al. (*BABAR* collaboration), [arXiv:0708.3650v1](https://arxiv.org/abs/0708.3650v1) [[hep-ex](#)], submitted to Phys. Rev. Lett.
- [28] R. D. Cousins, V. L. Highland, Nucl. Instr. Methods Phys. Res., Sect. A **320** (1992) 331
- [29] “The Discovery Potential of a Super B Factory”, SLAC-R-709 (2004); “Letter of Intent for KEK Super B Factory”, KEK Report 2004-4 (2004); “SuperB: A High-Luminosity Asymmetric  $e^+e^-$  Super Flavor Factory. Conceptual Design Report”, SLAC-R-856, INFN-AE-07-02, LAL-07-15 (2007).